Time evolution of damage in thermally induced creep rupture

2012 EPL 97 26006

(http://iopscience.iop.org/0295-5075/97/2/26006)

A Letters Journal Exploring the Frontiers of Physics

January 2012

EPL, **97** (2012) 26006
doi: 10.1209/0295-5075/97/26006

www.epljournal.org

Time evolution of damage in thermally induced creep rupture

N. Yoshioka[1], F. Kun[2(a)] and N. Ito[3]

[1] *Department of Theoretical Physics, University of Debrecen - H-4010 Debrecen, P.O. Box 5, Hungary, EU*
[2] *Yukawa Institute for Theoretical Physics, Kyoto University - Kitashirakawa Oiwake-cho, 606-8502 Kyoto, Japan*
[3] *Department of Applied Physics, Graduate School of Engineering, The University of Tokyo 7-3-1, Hongo, Bunkyo-ku, 113-8656 Tokyo, Japan*

received 2 November 2011; accepted in final form 9 December 2011
published online 18 January 2012

PACS 62.20.M- – Structural failure of materials
PACS 02.50.-r – Probability theory, stochastic processes, and statistics
PACS 05.90.+m – Other topics in statistical physics, thermodynamics, and nonlinear dynamical systems

Abstract – We investigate the time evolution of a bundle of fibers subject to a constant external load. Breaking events are initiated by thermally induced stress fluctuations followed by load redistribution which subsequently leads to an avalanche of breakings. We compare analytic results obtained in the mean-field limit to the computer simulations of localized load redistribution to reveal the effect of the range of interaction on the time evolution. Focusing on the waiting times between consecutive bursts we show that the time evolution has two distinct forms: at high load values the breaking process continuously accelerates towards macroscopic failure, however, for low loads and high enough temperatures the acceleration is preceded by a slow-down. Analyzing the structural entropy and the location of consecutive bursts we show that in the presence of stress concentration the early acceleration is the consequence of damage localization. The distribution of waiting times has a power law form with an exponent switching between 1 and 2 as the load and temperature are varied.

Motivations. – Under a constant external load materials typically exhibit a time-dependent macroscopic response and suffer failure after a finite time. Such creep rupture processes play a crucial role in technological applications limiting the lifetime of construction components [1]. Depending on the type of materials, creep rupture can have a wide variety of microscopic origins from the existence of frictional interfaces [1] through the viscoelasticity of the constituents [2], to thermally activated aging processes [3]. Recent investigations revealed the high importance of thermally activated micro-crack nucleation in creep phenomena [3–7] with consequences reaching even to geological scales [5].

Under the dominance of thermally activated damage accumulation, macroscopic failure often occurs as a sudden event following a short acceleration period. In spite of the smooth macroscopic evolution, on the micro-scale, thermally activated breakdown proceeds in bursts which may be exploited to gain information about the approach of the system to failure. In the present letter we investigate this problem in the framework of a fiber bundle model of thermally activated breakdown. Comparing analytical results obtained for equal load sharing to computer simulations performed in the limit of localized load redistribution we want to clarify the effect of the inhomogeneous stress field on the time evolution of the system. Analyzing the waiting times between consecutive bursts we show that depending on the temperature and external load the system is either continuously accelerating towards failure or, first slow-down occurs which is then followed by acceleration. We demonstrate that in the presence of stress concentrations the acceleration sets in earlier, which is the consequence of spatial localization of breaking bursts. We investigate the structural entropy and the consecutive positioning of bursts to quantify the localization of damage. The probability distribution of waiting times proved to have a power law functional form with an exponential cutoff in agreement with experimental findings. The value of the exponent switches from 1 to 2 as the temperature and the load are varied.

Homogeneous fiber bundle with thermal noise. – To investigate the role of thermal activation, several modeling approaches have been introduced which provided

(a) E-mail: feri@dtp.atomki.hu

a detailed understanding of the time dependence of breakdown phenomena [2,6,8–19]. To study the time evolution of thermally activated fracture processes, we follow the modeling approach of refs. [6,14,16,20]: we consider N parallel fibers on a square lattice of size L. The bundle is subject to a constant external load σ, under which the fibers have a linearly elastic behavior characterized by an identical Young modulus E. To take into account the effect of thermal noise in the fracture process, we assume that the local load on fibers $\sigma_i, i = 1, \ldots, N$ has time-dependent fluctuations $\xi(t)$ so that the load of fiber i at time t reads as

$$\sigma_i = \sigma_i^0 + \xi_i(t), \tag{1}$$

where σ_i^0 denotes the deterministic part arising from the external load and from the load transferred from broken fibers. The fibers break when the local load on them exceeds a threshold value $\sigma_i > \sigma_{th}$. It is a crucial feature of the model that the system is completely homogeneous, *i.e.* all the fibers have the same breaking strength $\sigma_{th} = 1$ so that the only source of fluctuations is the thermal noise arising due to the finite temperature T. Thermally induced stress fluctuations ξ are characterized by a Gaussian distribution with zero mean and a temperature-dependent standard deviation

$$p(\xi, T) = (1/\sqrt{2\pi T}) \exp(-\xi^2/2T). \tag{2}$$

The system evolves in discrete time steps sampling new values of ξ independently of each other.

After fiber breakings, the load of broken fibers has to be redistributed over the remaining intact ones. In this letter we consider two limiting cases for the range of load transfer: in the case of equal load sharing (ELS) all surviving fibers overtake equal fraction of the load. ELS ensures that the stress distribution remains homogenous in the bundle until the end of time evolution which also facilitates to perform analytical calculations. In the more realistic case of localized load sharing (LLS) the load of a broken fiber is equally distributed over its intact nearest neighbors in the square lattice resulting in a high stress concentration along the perimeter of failed regions.

In spite of its simplicity, analytical and numerical investigation of this FBM provided a deep insight into the process of thermally activated creep rupture [6,7,14–16]. When the load is redistributed equally it has been found that the lifetime t_f of the bundle has an Arrhenius type dependence on the temperature T and on the load σ [6,16]. For localized load sharing (LLS) an anomalous scaling of t_f was revealed with the system size N [14,15]. Analyzing the microstructure of damage in the last stable state of the system under LLS, it was shown that besides the usual Griffith type of abrupt rupture, a disorder-dominated regime emerges where fracture proceeds slowly. It was pointed out that the phase boundary is the Kertész-line of the system, well known in the theory of phase transitions [15]. On the macro-level the time evolution of strain in the model has been studied in refs. [5,6,13]

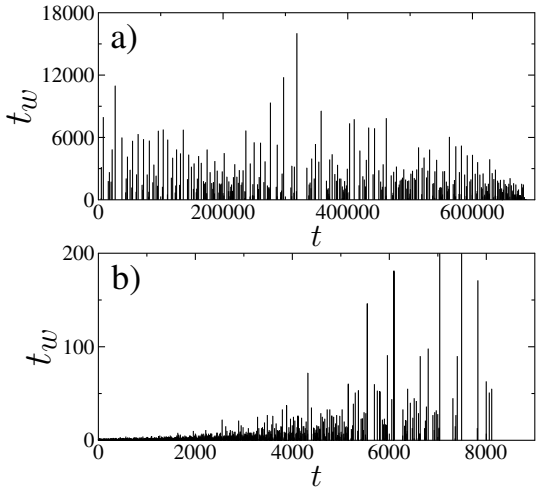

Fig. 1: Waiting times t_w following an avalanche plotted at the time t where the avalanche occurred. The parameter values are $T = 0.03$, $\sigma = 0.1$ (a) and $T = 0.1$, $\sigma = 0.0001$ (b). It can be observed that at high load (a) the system accelerates when approaching macroscopic failure, however, at low load (b) the waiting times increase indicating the slowing-down of breakings. Note that a relatively small system $L = 64$ is used for demonstration purposes in order not to have too many bursts.

in qualitative agreement with experiments. However, the effect of the lateral deformation of fibers caused by the collapse of neighboring ones, that may be relevant for real fibrous structures, is not captured in the model.

Waiting times between bursts of breakings. – On the micro-level, the fibers primarily break due to thermal fluctuations when their actual load exceeds the fixed breaking threshold $\sigma_i(t) > \sigma_{th}$. Of course, depending on the temperature in a given time step more than one fiber can break at the same time. The load of broken fibers is then redistributed over the intact ones according to the selected load sharing rule. The load increments on intact fibers can trigger additional breakings and eventually generate an entire breaking burst. The size of the burst $\Delta(t)$ occurring at time t is simply the number of fibers breaking in the burst. Hence, irrespective of the range of load sharing the failure of the bundle proceeds in bursts which are separated by silent periods with no breakings.

In our FBM the waiting time t_w is defined as the number of iteration steps without breakings between two consecutive avalanches. In the present letter we focus on the time evolution of the system analyzing the statistics of waiting times t_w and their relation to the microstructure of damage. Figure 1 presents the waiting times t_w elapsed from an avalanche until the next one in a fiber bundle with equal load sharing. The value of t_w is plotted at the time when the first avalanche occurred. It can be observed that the waiting times strongly fluctuate over a broad range. It is interesting to note that at high load values (fig. 1(a)) the waiting times decrease as the system approaches macroscopic failure. This demonstrates that

the load increments generated by bursts give rise to an acceleration of the breaking process when approaching failure. However, at low external load (fig. 1(b)) avalanches cannot have a significant triggering effect, the failure process is dominated by thermal noise until the end. Since the number of intact fibers $N(t)$ is a monotonically decreasing function of time, as the system evolves thermal fluctuations have less chance to initiate avalanches.

Under equal-load-sharing conditions the state of the evolving system is fully characterized by the number of intact fibers $N(t)$ from which the fraction of broken ones ϕ can be obtained as $\phi = 1 - N(t)/N$. After an avalanche stopped, the probability p_1 that a randomly selected fiber does not break over time t_w is

$$p_1(t_w, \phi) = [1 - P(\sigma_{th} - \sigma(\phi), T)]^{t_w}, \qquad (3)$$

where the load of single fibers $\sigma(\phi)$ follows from the condition of equal load sharing $\sigma(\phi) = \sigma/(1-\phi)$ and P denotes the complementary cumulative distribution of thermal fluctuations eq. (2). Due to the independence of thermally induced fiber failures, the probability p that the entire bundle survives the time t_w reads as

$$p(t_w, \phi) = [1 - P(\sigma_{th} - \sigma(\phi), T)]^{N(1-\phi)t_w}, \qquad (4)$$

where $N(1-\phi)$ is the number of intact fibers. The complementary cumulative distribution $p(t_w, \phi)$ can be cast into a simple exponential form $p(t_w, \phi) = e^{-\lambda t_w}$, with $\lambda = 1/\langle t_w(\phi)\rangle$. Here $\langle t_w(\phi)\rangle$ denotes the average value of waiting times

$$\langle t_w(\phi)\rangle = \int_0^\infty p(t, \phi)\, \mathrm{d}t, \qquad (5)$$

which yields the form

$$\langle t_w(\phi)\rangle = -\frac{1}{N(1-\phi)\ln[1 - P(\sigma_{th} - \sigma(\phi), T)]}. \qquad (6)$$

Note that the value of ϕ can vary from 0 to the critical value $\phi_c^{ELS} = 1 - \sigma/\sigma_{th}$, where catastrophic collapse occurs. The functional form of $\langle t_w(\phi)\rangle$ is illustrated in fig. 2 for the fixed temperature $T = 0.1$ varying the external load σ in a broad range. It follows from eq. (6) that for zero load $\sigma = 0$ the average waiting time $\langle t_w(\phi)\rangle$ monotonically increases and has a power law divergence

$$\langle t_w(\phi)\rangle \sim (1-\phi)^{-1} \qquad (7)$$

as ϕ approaches the zero load critical value $\phi_c^{ELS} = 1$. The result implies that in this limiting case the fracture process slows down with increasing time as it has been observed in fig. 2. Since the system is purely driven by thermal fluctuations, one has to wait longer to obtain the next breaking event when less and less fibers remain available for breaking. It can be observed in the figure that increasing the external load σ the $\langle t_w(\phi)\rangle$ curves develop a maximum, which then gradually disappears and for high load values the average waiting time becomes a monotonically decreasing function of ϕ. The position of the maximum ϕ_m marks an important configuration of the system

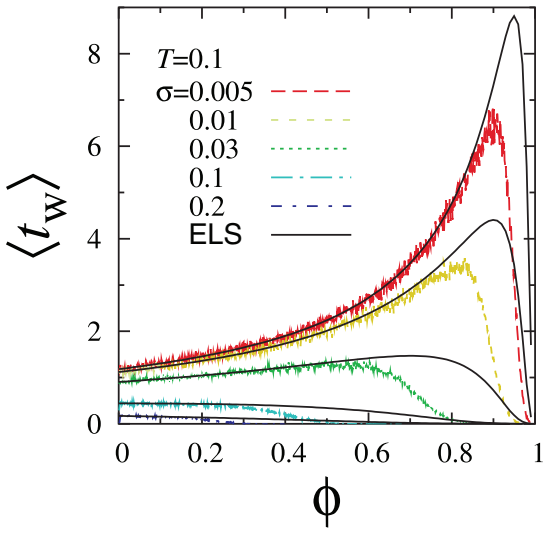

Fig. 2: (Color online) Average waiting time $\langle t_w(\phi)\rangle$ as a function of ϕ in ELS and LLS FBMs for a fixed temperature $T = 0.1$ varying the external load in a broad range. The ELS curves were obtained from eq. (6).

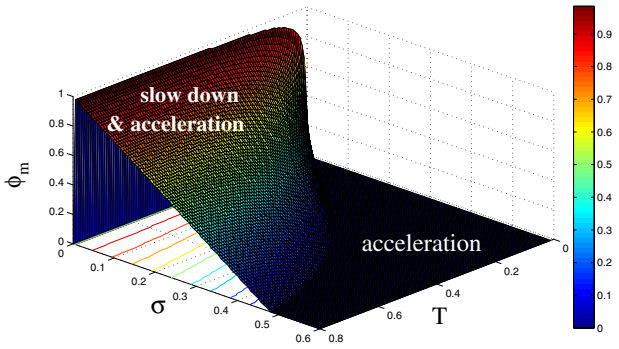

Fig. 3: (Color online) Position of the maximum ϕ_m of the average waiting time $\langle t_w\rangle$ as a function of temperature T and applied load σ for equal load sharing. The color code represents the value of ϕ_m. The broad parameter range with $\phi_m = 0$ indicates the phase where the system always accelerates.

where the breaking process starts to accelerate towards macroscopic failure. The emergence of the accelerating phase indicates that for $\phi > \phi_m$ the increased load on single fibers $\sigma/(1-\phi)$ becomes sufficient to compensate the effect of the decreasing number of intact fibers $N(t)$. Starting from eq. (6) we determined numerically the value of ϕ_m as a function of temperature T and external load σ (see fig. 3). The calculations showed that for high enough loads $\sigma \gtrsim 0.487$ the fracture process continuously accelerates. However, at lower load values the acceleration phase is preceded by a slowing-down over a broad temperature range.

Simulations have shown that localized load sharing (LLS) results in a faster time evolution of the system, *i.e.* the lifetime of LLS bundles is always lower than their ELS counterparts $t_f^{LLS} < t_f^{ELS}$ [14,15]. To obtain a more

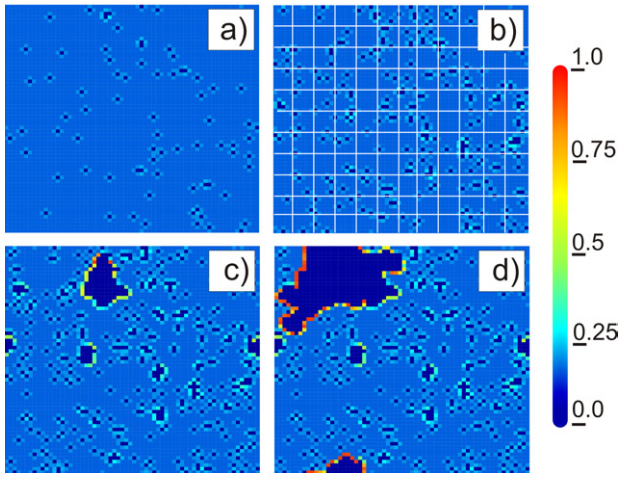

Fig. 4: (Color online) Time evolution of a sample of size $L=64$ at the temperature $T=0.03$ and load $\sigma=0.1$ values. The lifetime of the system is $t_f=787159$. The snapshots are taken at times $t=100000$ (a), $t=400000$ (b), $t=680000$ (c), $t=787159$ (d). The color code represent the load of fibers with the maximum $\sigma_{th}=1$. Deep blue indicates broken fibers (zero load), which form clusters (cracks). Along the perimeter of cracks high stress concentration builds up. The mesh in (b) illustrates the calculation of the structural entropy.

detailed picture of the effect of the range of load sharing, in fig. 2 the average waiting times of ELS and LLS bundles are compared. It can be observed that the $\langle t_w(\phi)\rangle$ curves have the same functional form in both cases, however, for LLS the acceleration towards macroscopic failure sets in earlier, *i.e.* at lower fraction of broken fibers ϕ. Large-scale computer simulations revealed that the phase boundary in fig. 3 separating the continuously accelerating phase from the one where slow-down precedes acceleration coincides for LLS and ELS bundles. The difference is that the value of ϕ_m is significantly lower for LLS systems $0 \leqslant \phi_m^{LLS} < \phi_m^{ELS}$. In order to understand how the inhomogeneous stress field gives rise to the early acceleration of the creeping system we analyze the microstructure of damage.

Spatial structure of damage. – When the load sharing is localized a complex breaking scenario arises as a result of the competition of breakings due to thermal noise and due to stress enhancements around failed regions. At the beginning of the breaking process there is no significant difference between ELS and LLS systems due to the dominance of thermal noise, hence, the $\langle t_w(\phi)\rangle$ curves follow each other in fig. 2 for low values of ϕ. The time evolution of the spatial structure of damage is illustrated in fig. 4 for a system of size $L=64$ with localized load sharing, which is intentionally chosen to be small to observe the details of the cluster structure. It can be seen that at the beginning of time evolution single broken fibers nucleate in the lattice in a completely uncorrelated manner (fig. 4(a)). Right after the first time step the structure of the lattice is analogous to a percolation lattice with the occupation probability $p_b = P(\sigma_{th}-\sigma, T)$. As time elapses more nucleations occur (fig. 4(b)) but also small broken clusters have an enhanced chance to expand by the breaking of highly stressed fibers along the cluster boundaries (fig. 4(c)). As the stress concentration increases at the cluster boundaries due to the gradual growth of clusters, the probability of fiber breaking becomes much higher along clusters then inside intact regions, where fibers experience only the remote load σ. As a consequence, instead of nucleation of new clusters, the growth of already existing ones will dominate as time elapses (see figs. 4(b), (c)). It can be observed in fig. 4(c) that several clusters grow at the same time, however, in (d) one of the clusters gets selected which then rapidly expands. Note that snapshots are always taken in stable configurations between avalanches. Figure 4(d) presents the last stable configuration of the system in which a single fiber breaking initiates an unstable growth of the dominating cluster.

To characterize the effect of spatial localization of breaking events on the time evolution of the system, we analyzed how the spatial extension of avalanches and their consecutive position evolve as the system approaches macroscopic failure. Since the creep rupture process is driven by thermal fluctuations of the local stress, fibers breaking in spatially disconnected regions of the bundle may contribute to the same avalanche even if the load sharing is localized. To quantify the spatial extension of avalanches we calculated the structural entropy S of fibers breakings in individual avalanches. The method we apply is somewhat similar to the technique which was introduced in ref. [21] to analyze the spatial structure of acoustic emissions in rupture experiments: For the calculation of the entropy a rectangular mesh is placed on the sample (see fig. 4(b)) and we count the number of fibers n_i of an avalanche of size Δ breaking inside the plaquette i. The structural entropy S is defined as

$$S = -\sum_i q_i \ln q_i, \tag{8}$$

where $q_i = n_i/\Delta$ is the fraction of fibers of the avalanche in plaquette i. The value of S is normalized by the entropy S_u corresponding to the uniform distribution of Δ number of broken fibers. For the specific calculations the mesh size was chosen to be 4×4 fibers. The behavior of the structural entropy S is compared to the average waiting time $\langle t_w\rangle$ in fig. 5 as a function of ϕ. It can be observed in the figure that for localized load sharing the value of S remains constant and has a high value $S\approx 0.8$ during the regime of slow-down, which shows that spatially disconnected regions participate in avalanches. However, beyond the maximum ϕ_m of $\langle t_w\rangle$ the entropy S rapidly decreases to zero as macroscopic failure is approached. This implies the strong spatial localization of avalanches, *i.e.* fibers breaking in an avalanche are bounded to small spatial regions. Comparing to fig. 4 it can be noted that in the decreasing regimes of S the breaking events mainly

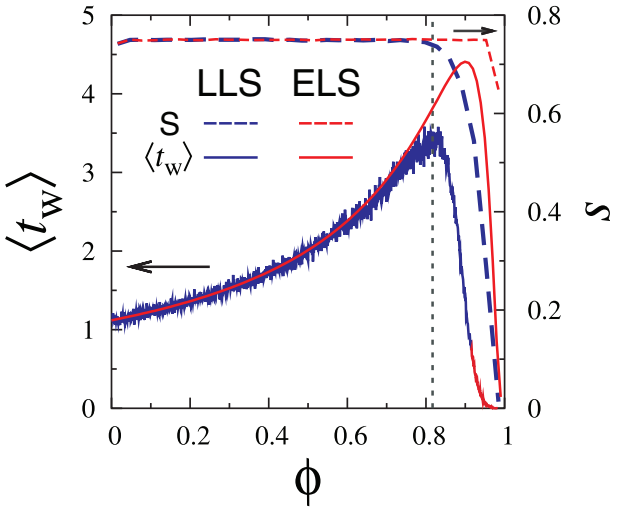

Fig. 5: (Color online) Comparison of the structural entropy S and the average waiting time $\langle t_w \rangle$ as a function of ϕ for ELS and LLS bundles at $T = 0.1$ and $\sigma = 0.01$. It can be observed that for ELS no localization occurs, while for LLS strong localization emerges which is accompanied by the acceleration of the dynamics. The vertical dotted line shows ϕ_m for LLS.

occur along the perimeter of clusters resulting in growth. It is important to emphasize that as localization sets on the dynamics of the system accelerates, *i.e.* the decreasing entropy is accompanied by the decrease of the average waiting time. Note that the effect is missing for ELS systems: in the absence of stress concentration the entropy remains high $S \approx 0.6$–0.8 until the end of the process, which clearly shows that the acceleration towards failure in ELS is not related to the spatial evolution of damage as it is expected. Simulations revealed that in the phase of continuous acceleration both $\langle t_w \rangle$ and S monotonically decrease (not shown in the figure for clarity).

Figure 6 presents the position of the center of mass of bursts in a bundle of size $L = 256$ at the same temperature and load value as in fig. 4. It is important to emphasize that small-sized bursts are homogeneously spread over the system, however, as global rupture is approached the events get clustered, *i.e.* the last few hundred avalanches occur in a small region (indicated by the circle in the figure) compared to the system size L. Additionally, these avalanches have the largest size Δ, although their spatial extension is small characterized by the low value of the structural entropy $S \approx 0$. This strong localization plays a dominating role in the final stage of the rupture process.

Waiting time distributions. – The probability distribution of waiting times $D(t_w)$ proved to be sensitive to the value of load and temperature. For equal load sharing the waiting time distribution $D(t_w)$ can be obtained analytically in the limiting case of zero external load $\sigma = 0$: For very large system sizes $N \to \infty$ the waiting time has low fluctuations so that it can be well represented by its average $t_w(\phi) \sim \langle t_w(\phi) \rangle$, where $\langle t_w(\phi) \rangle$ is given by

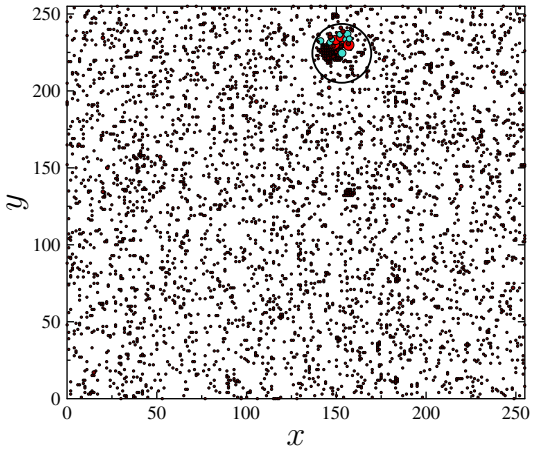

Fig. 6: (Color online) Position of the center of mass of avalanches in a bundle of size $L = 256$. Until macroscopic failure 3915 avalanches appeared. The circle shows the region where the last 250 avalanches fall. The size of spots is proportional to the logarithm of the avalanche size Δ supported by the color code: $\Delta = 1$–5 (black), $\Delta = 5$–15 (green), and $\Delta > 15$ (red).

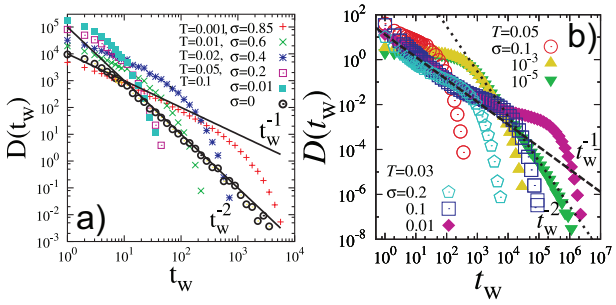

Fig. 7: (Color online) Waiting time distributions for (a) equal and (b) localized load sharing FBMs obtained at different load and temperature values. The straight lines present power laws with exponent $z = 1$ and $z = 2$ to guide the eye.

eq. (7) for $\sigma = 0$. Since $\langle t_w(\phi) \rangle$ is a monotonous function of ϕ, the probability density function $D(t_w)$ of waiting times has the feature $D(t_w)dt_w \sim d\phi$. Substituting eq. (7), a power law functional form is obtained:

$$D(t_w) \sim t_w^{-z}, \tag{9}$$

where the exponent $z = 2$ is independent of the temperature T. Waiting time distributions of ELS fiber bundles are presented in fig. 7(a) where a perfect agreement of the analytic prediction and of the numerical results is observed at $\sigma = 0$. The waiting time distributions $D(t_w)$ of local load sharing FBMs can only be evaluated by numerical means. At low load values $\sigma \to 0$ the inhomogeneous stress field has no relevant effect, hence, in fig. 7(b) the distributions $D(t_w)$ tend to the ELS power law with exponent $z = 2$. In fig. 7 temperature T and load σ values are selected to have $D(t_w)$ curves from the regimes of continuous acceleration and slow-down→acceleration for both ELS and LLS bundles. Comparing the ELS and LLS

distributions the remarkable feature is that in the continuously accelerating phase power laws are always obtained with exponent $z = 1$ independent of the range of load sharing. In the slow-down regime the functional form of $D(t_w)$ gradually changes from a power law of exponent $z = 2$ at low loads, to another one with exponent $z = 1$ followed by an exponential cutoff. It can be observed in the figure that as the load and the temperature are increased the power law regime gets narrower and the distribution has a crossover to a purely exponential form. It has to be emphasized that the waiting time distributions are in a good qualitative agreement with recent experimental findings on thermally activated rupture processes [3,6,7,22].

Discussion. – We investigated the time evolution of damage during the creep rupture process of a fiber bundle which is driven by thermally induced local stress fluctuations. The analytic results obtained in the limit of equal load sharing served as a reference to clarify the effect of spatial correlations on the fracture process in comparison to computer simulations of localized load sharing.

Analyzing the waiting times between consecutive bursts of fiber breakings, we showed that the creeping process evolves in two possible forms: at high load values the process continuously accelerates towards macroscopic failure, however, at low loads and high enough temperatures the acceleration is preceded by a slow-down process. When the load is equally distributed in the system, the competition of the decreasing number of intact fibers available for breaking and of the increasing load on intact fibers leads to the emergence of the two phases. In the case of localized load sharing, the stress concentration around cracks leads to spatial correlation of breaking events and to an enhanced breaking probability which in turn gives rise to an early acceleration.

In order to quantify the effect of spatial correlation on the time evolution of the creep rupture process, we evaluated the structural entropy of avalanches and their consecutive positioning. As a very important outcome, our calculations revealed that the decreasing extension and the spatial localization of avalanches to a bounded region of the specimen is responsible for the acceleration towards macroscopic failure. Final failure is driven by a single growing crack which becomes unstable. The waiting time distributions have a power law behavior with an exponential cutoff, where the exponent switches from 1 to 2 as the load and temperature are varied.

* * *

The work is supported by TAMOP-4.2.1/B-09/1/KONV-2010-0007 project. The project is implemented through the New Hungary Development Plan, co-financed by the European Social Fund and the European Regional Development Fund. FK acknowledges the support of OTKA K84157 and of the Bólyai János foundation of the HAS. This work was supported by the European Commissions by the Complexity-NET pilot project LOCAT. This work was partly supported by the MTA-JSPS program, by JP-24/2009 and by the Global Research Partnership program of KAUST (KUK-I1-005-04). This work is partially supported by Grant-in-Aid for JSPS Fellows.

REFERENCES

[1] Suresh S., *Fatigue of Materials* (Cambridge University Press) 1998.
[2] Kun F., Moreno Y., Hidalgo R. C. and Herrmann H. J., *Europhys. Lett.*, **63** (2003) 347.
[3] Nechad H., Helmstetter A., Guerjouma R. E. and Sornette D., *Phys. Rev. Lett.*, **94** (2005) 045501.
[4] Bonn D., Kellay H., Prochnow M., Ben-Djemiaa K. and Meunier J., *Science*, **280** (1998) 265.
[5] Sornette D. and Ouillon G., *Phys. Rev. Lett.*, **94** (2005) 038501.
[6] Guarino A., Garcimartin A. and Ciliberto S., *Europhys. Lett.*, **47** (1999) 456.
[7] Garcimartn A., Guarino A., Bellon L. and Ciliberto S., *Phys. Rev. Lett.*, **79** (1997) 3202.
[8] Curtin W. A., Pamel M. and Scher H., *Phys. Rev. B*, **55** (1997) 12051.
[9] Newman W. I. and Phoenix S. L., *Phys. Rev. E*, **63** (2001) 021507.
[10] Phoenix S. L. and Newman W. I., *Phys. Rev. E*, **80** (2009) 066115.
[11] Bazant Z. P. and Pang S., *J. Mech. Phys. Solids*, **55** (2007) 91.
[12] Hidalgo R. C., Kun F. and Herrmann H. J., *Phys. Rev. E*, **65** (2002) 032502.
[13] Scorretti R., Ciliberto S. and Guarino A., *Europhys. Lett.*, **55** (2001) 626.
[14] Yoshioka N., Kun F. and Ito N., *Phys. Rev. Lett.*, **101** (2008) 145502.
[15] Yoshioka N., Kun F. and Ito N., *Phys. Rev. E*, **82** (2010) 055102.
[16] Roux S., *Phys. Rev. E*, **62** (2000) 6164.
[17] Pradhan S., Hansen A. and Chakrabarti B. K., *Rev. Mod. Phys.*, **82** (2010) 499.
[18] Jagla E. A., *Phys. Rev. E*, **83** (2011) 046119.
[19] Kovacs K., Nagy S., Kun F., Herrmann H. J. and Pagonabarraga I., *Phys. Rev. E*, **77** (2008) 036102.
[20] Politi A., Ciliberto S. and Scorretti R., *Phys. Rev. E*, **66** (2002) 026107.
[21] Guarino A., Garcimartin A. and Ciliberto S., *Eur. Phys. J. B*, **6** (1998) 13.
[22] Maes C., van Moffaert A., Frederix H. and Strauven H., *Phys. Rev. B*, **57** (1998) 4987.